Nyman, Leo; Pudas, Marko; Aab, Kaisa; Sammelselg, Väino; Kukli, Kaupo; Alles, Harry; Netšipailo, Ivan; Mäeorg, Uno; Wessing, Johanna; Suliga, Adnieszka; Tighe, Adrian; Merisalu, Maido; Manninen, Emmi

Coatings Made by Atomic Layer Deposition for the Protectionof Materials from Atomic Oxygen in Space

Published in:
IOP Conference Series: Materials Science and Engineering

Published: 01/01/2023

Document Version
Publisher's PDF, also known as Version of record

Please cite the original version:
Nyman, L., Pudas, M., Aab, K., Sammelselg, V., Kukli, K., Alles, H., Netšipailo, I., Mäeorg, U., Wessing, J., Suliga, A., Tighe, A., Merisalu, M., & Manninen, E. (2023). Coatings Made by Atomic Layer Deposition for the Protectionof Materials from Atomic Oxygen in Space. *IOP Conference Series: Materials Science and Engineering*, *1287* . http://10.1088/1757-899X/1287/1/012014

IOP Conference Series: Materials Science and Engineering

Coatings Made by Atomic Layer Deposition for the Protection of Materials from Atomic Oxygen in Space

To cite this article: Maido Merisalu *et al* 2023 *IOP Conf. Ser.: Mater. Sci. Eng.* **1287** 012014

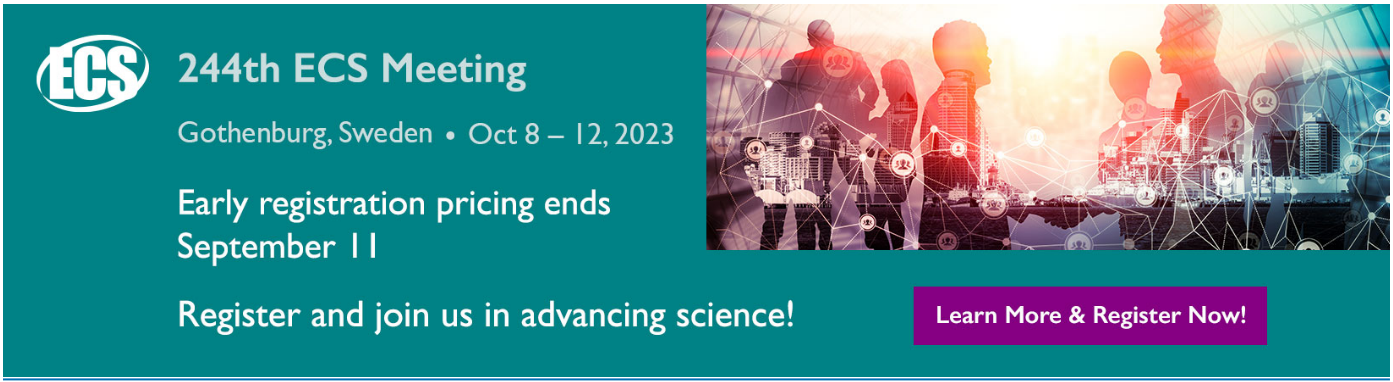

Coatings Made by Atomic Layer Deposition for the Protection of Materials from Atomic Oxygen in Space

Maido Merisalu[1], Kaisa Aab[1], Väino Sammelselg[1], Kaupo Kukli[1], Harry Alles[1], Ivan Netšipailo[1], Uno Mäeorg[2], Johanna Wessing[3], Agnieszka Suliga[3], Adrian Tighe[3], Leo Nyman[4], Marko Pudas[5], Emmi Manninen[5]

[1]Institute of Physics, University of Tartu, W. Ostwaldi 1, 50411 Tartu, Estonia
[2]Institute of Chemistry, University of Tartu, Ravila 14a, 50411 Tartu, Estonia
[3]European Space Research and Technology Centre – ESTEC, Materials' Physics & Chemistry Section. TEC-QEE, Keplerlaan 1, 2201 AZ Noordwijk, The Netherlands
[4]Aalto University - School of Electrical Engineering, Department of Electronics and Nanoengineering - Space Science, 02150 Espoo, Finland
[5]Picosun Oy, Masalantie 365 02430 Masala, Finland

maido.merisalu@ut.ee

Abstract. Atomic Layer Deposition (ALD) has been investigated for the possible protection of various materials against atomic oxygen (ATOX) at ESTEC Materials and Electrical Components Laboratory facility. ALD is a conformal coating process, that can be used to apply ultra-thin films of metal oxides on various materials, that may have a sophisticated three-dimensional shape, such as the internal and external components of satellites. The challenge with metal oxides on soft and/or flexible surfaces arises from the brittle nature of these ceramic films if their thickness exceeds 30 nm. Different substrates, including silicon, Printed Circuitry Board (PCB), polyimide, and Carbon Fibre Reinforced Polymers (CFRP) were coated by ALD with 20 nm thick metal oxide films at 125 °C, then exposed to ATOX and characterized by photographing, reflectance measurement and scanning electron microscopy (SEM). The studies showed good performance of protective films prepared by ALD on polymer substrates, which suggests that the nanometer-scale coatings can improve the lifetime of these materials at low Earth orbit, where they are inevitably exposed to ATOX. In contrast, the uncoated substrates suffered near-surface damage after exposure to ATOX, which resulted in microscopic features on their surface that were visible in SEM. Damage caused by ATOX to the uncoated substrates was also visible in photographs and observable in reflectance studies. In the latter case, the changes in the reflectance spectrum were caused by the change of surface morphology and/or chemical and elemental composition due to corrosion by ATOX.

1. Introduction

The environment in low Earth orbit (LEO) is particularly corrosive for some materials due to the presence of energetic atomic oxygen [1]. Therefore, corrosion tests have been performed over the last decades at the International Space Station [2,3], as well as in laboratory conditions [4] in order to assess the performance of materials for possible use in LEO. These studies have shown that certain metals (e.g. silver) and organic materials are particularly vulnerable to corrosion caused by atomic oxygen and should not be directly exposed to the environment of space. Therefore, the list of materials for safe use in space is actually quite short and testing, although costly, is necessary to implement new ones.

A possible solution to the latter problem may be atomic layer deposition (ALD) of solid material layers, which was already investigated for its potential for corrosion protection in 1999 [5]. The greatest advantage of ALD over other coating preparation technologies is the fact that it allows one to uniformly coat substrates that may have a sophisticated three-dimensional shape [6]. A recent study has also demonstrated that some metal oxide coatings are barely affected by atomic oxygen and may thus provide excellent corrosion resistance at LEO [7]. In the latter study [7], only the top layer of the coating (~10 nm TiO_2) was slightly modified during testing with atomic oxygen, which could be regarded as equivalent to one year of exposure to atomic oxygen at LEO, i.e., at an altitude that is comparable to that of the International Space Station (~400 km). In another paper, plasma-enhanced chemical vapor deposition (PECVD) was used to prepare a functional coating, which also had a TiO_x top layer and provided excellent protection against atomic oxygen [8]. Furthermore, the ceramic coatings grown by ALD onto polymer-based substrates can reduce outgassing [9] which is problematic for sensitive instruments used for satellites. However, such coatings need to be grown to thicknesses below 30 nm [10]. Namely, in a recent study [10] it was shown thinner ceramic films grown by ALD have a higher critical tensile and compressive strains which would reduce the risk of coating failure on flexible substrates such as polymers.

In the present study, we report the possibility of using thin ceramic coatings prepared by ALD to enhance the corrosion resistance of various polymer-based materials and flexible substrates against atomic oxygen.

2. Experimental

2.1. Sample preparation

The experiments in this work were done with uncoated and coated 20 × 20 mm^2 substrates: silicon (Si, manually cut from prime P-type silicon wafer), polyimide (Kapton HN, DuPont), carbon fiber reinforce polymer (CFRP, provided by the German Aerospace Center, DLR), a printed circuit board (PCB, manufactured from ISOLA Group's 370HR, 180°C glass transition temperature FR-4 by Aspocomp Oy) and polymer film infrared Fresnel window (IRW, Edmund Optics). The substrates were, prior to the film growth, examined to detect the presence of dust particles and evaluate the smoothness of surface for uniform coating. The samples were cleaned with pressurized air to remove loose dust particles. Additional cleaning was performed with isopropanol, followed by drying in a laminar flow cabinet. The ceramic coating of 20 nm thickness was applied by ALD in a commercial reactor P300 (Picosun Oy, an Applied Materials Company), using the coating recipe which was provided with the instrument.

2.2. Testing with atomic oxygen

Atomic oxygen testing was performed at the low Earth orbit simulation facility (LEOX) based on the Laser Pulse Induced Breakdown (LPIB) principle in ESA's Materials & Electrical Components Laboratory [4]. The experimental atomic oxygen fluence was comparable to approximately 1 year of exposure of a direct flux of atomic oxygen at the altitude of the International Space Station at an average of 400 km. The precise values of fluence for each sample slot are given in Table 1. Prior to the main test, pre-tests were performed to measure the average flux and the spread in atomic oxygen flux across the sample plate calculated from the mass loss of Kapton witnesses. To control the adsorbed and absorbed moisture, all samples were placed in a conditioning cabinet for at least 24h before the mass measurements using a Sartorius ME5 micro balance. For the main test, the samples were weighed and photographed before (BOT) and after (EOT) the exposure, as well as characterized thoroughly with various techniques that will be described in the Section 2.3 below.

Table 1. Atomic oxygen fluence (atoms/cm^2) for tested substrates.

Substrate	**Coating**	**Fluence (atoms/cm^2)**
Polyimide (Kapton HN)	-	2.28E+21
Polyimide (Kapton HN)	ALD	2.35E+21
Carbon fiber reinforced polymer	-	2.86E+21
Carbon fiber reinforced polymer	ALD	2.86E+21
Printed circuit board	-	1.53E+21
Printed circuit board	ALD	1.20E+21
Polyethylene (infrared window)	-	8.82E+20
Polyethylene (infrared window)	ALD	1.04E+21
Silicon (1)	ALD	2.06E+21
Silicon (2)	ALD	2.23E+21

2.3. Surface characterization

The surfaces of the samples were inspected visually for discoloration using digital photography (Canon EOS 550D/Canon EOS 700D) with a stand and a macro lens. High resolution scanning electron microscopy (HR-SEM) studies and localized elemental analysis on most of the substrates were carried out with Helios Nanolab 600 (FEI Company) microscope that was equipped with an energy-dispersive X-ray spectrometry (EDX) analyzer INCA Energy 350 (Oxford Instruments) for X-ray microanalysis. Additional elemental analysis was done with a wavelength-dispersive X-ray fluorescence spectrometer (WD-XRF) ZSX 400 (Rigaku). The roughness of coatings on Si substrates was studied with an atomic force microscope AutoProbe CP II (Park SI/Veeco) in non-contact mode. The thickness of the ALD coatings was measured with ellipsometer SE-2000 (Semilab). The solar absorptance, α, and total optical reflectance in the spectral range of 250 – 2500 nm were analyzed, using a Cary 5000A (Agilent) spectrometer. The fourier transformation infrared (FT-IR) spectroscopy studies were performed with a Nicolet 6700 FT-IR spectrometer (Thermo Scientific) that was equipped with a Smart Orbit diamond micro-ATR accessory (refractive index of 2.4, active sample area diameter of 1.5 mm and angle of incidence of 45°). The spectrometer has DLaTGS detector, Vectra Aluminum Interferometer, a sealed and desiccated optical bench with CsI optics. The FT-IR spectrometer was protected from atmospheric moisture by constant purging with dry air.

3. Results

3.1. The effect of energetic atomic oxygen on the uncoated materials

The digital photos and SEM images of uncoated polyimide, CFRP, PCB and an IR-window material samples are depicted in Fig. 1. Visual inspection and photographs of the samples (Fig. 1a–d) showed that exposure to atomic oxygen had an impact on the surface of these materials. The circular unmasked area, which was directly exposed to the flux of atomic oxygen, could be clearly distinguished on all samples. A more detailed analysis with SEM provided insights into the damaging surface effects caused by ATOX. (Fig. 1e–l). SEM studies of polyimide (Fig. 1e,i) showed that the tested area was eroded rather uniformly and resulted in a rough topography with cavities that had a diameter of a few hundred nanometers. SEM studies of the CFRP substrate revealed that atomic oxygen had caused damage to both the carbon fibers (Fig. 1f,j) as well as the binding polymer (not shown). In this case, the fibers (Fig. 1j) appeared to be smoother than polyimide (Fig. 1i) after exposure to atomic oxygen. On the PCB substrate, SEM studies demonstrated minor damage to the metal area (Fig. 1g,k) and moderate damage, similar to polyimide and CFRP, on the green support material (not shown). SEM studies of the IR-window material on the other hand showed that the exposure to atomic oxygen resulted in the formation of micrometric cavities which were filled with semi-loose nanoparticles (Fig. 1h,l). The carpet-like structure caused by ATOX as observed in Fig. 1i,j,l had been described in an earlier study on polymer materials as a typical ATOX effect [11].

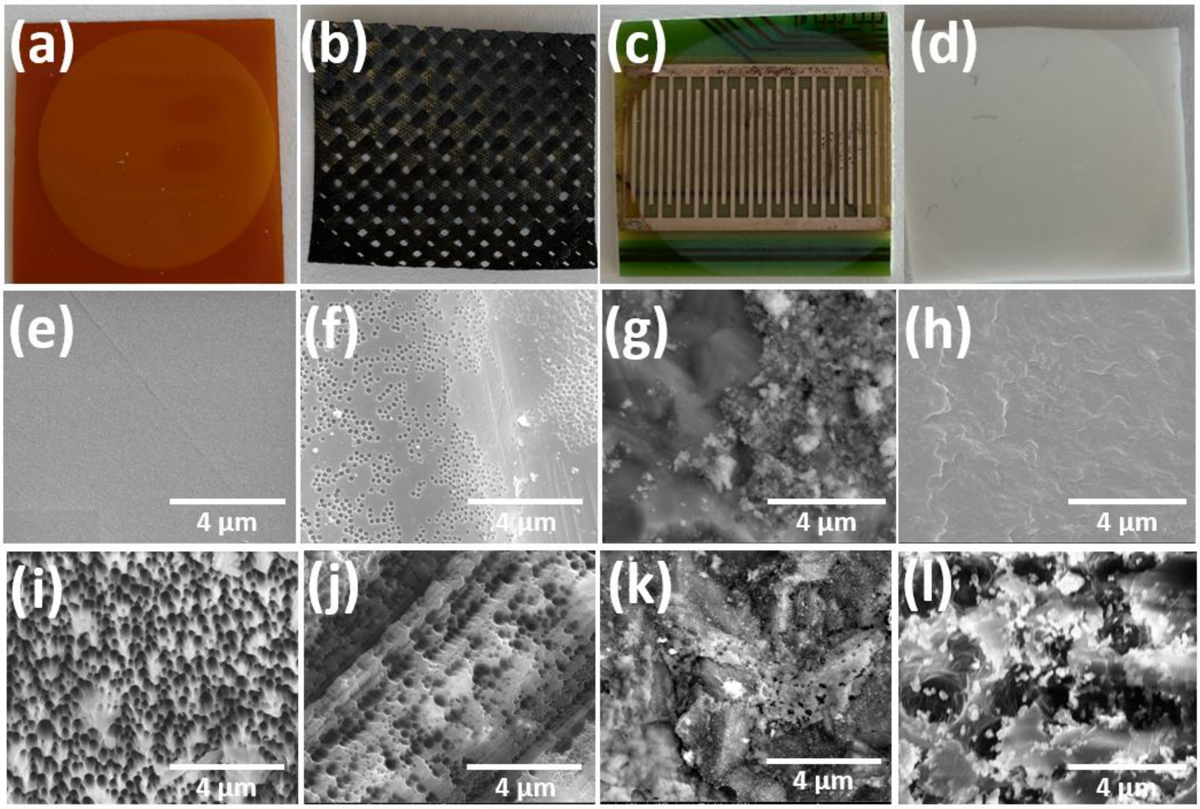

Figure 1. Photos (a-d) and HR-SEM images (e-l) of polyimide (a,e,i), CFRP (b,f,j), PCB (c,g,k) and IRW (d,h,l) before (e-h) and after (i-l)) atomic oxygen test. On PCB, the HR-SEM images (g,k) were made of the metal part.

The mass measurements of polyimide, CFRP, PCB and the IR-window film (Table 2) before and after exposure to atomic oxygen are in good agreement with the photos and HR-SEM studies depicted in Fig. 1. The highest mass erosion was observed for polyimide, which also exhibits a visual change of appearance in the photo (Fig. 1a). Another substrate with high mass erosion was CFRP (Fig. 1b, Table 2), which had suffered damage both to the polymer and carbon fibers (Fig. 1j). The PCB exhibited the lowest mass erosion value, which coincides with the HR-SEM studies. Namely, the PCB is mostly covered with metal, which suffered only minor damage (Fig. 1k) in comparison with the green support. The IR-window material was eroded less than polyimide and CFRP (Table 2), which is also in agreement with the visual observation and photos in Fig. 1a,b,d.

Table 2. Mass measurements of uncoated substrates before and after exposure to atomic oxygen.

Measured parameters	**Materials**			
	Polyimide	**CFRP**	**PCB**	**IRW**
Mass before test (mg)	88.712	58.596	1080.473	138.283
Mass after test (mg)	60.478	42.555	1077.040	132.500
Erosion (mg; %)	28.234 (31.8%)[b]	16.041 (27.4%)	3.433 (0.3%)	5.783 (4.2%)
Fluence (Atoms/cm^2; %)	2.28E+21 (259%)	2.86E+21 (324%)	1.53E+21 (173%)	8.82E+20 (100%)[a]

[a] Normalization of the fluence level: the fluence for IRW is taken as 100 %.
[b] Normalized erosion.

The corrosion mechanisms of polyimide and polyethylene were studied further by infrared spectroscopy (Fig. 2) and elemental analysis by XRF and SEM-EDX (Table 3). The IR spectrums measured before and after ATOX exposure were nearly identical in shape but differed in overall transmittance. In particular, the exposure to ATOX had increased the transmittance, which can be explained by the increase of surface roughness as observed in Fig. 1e,h. Such an increase of surface roughness effectively reduces the density of the material in the surface layer, which also reduces the optical path and therefore contributes to the increase in transmittance. Furthermore, IR spectroscopy studies showed that exposure to ATOX did not introduce characteristic changes in the individual absorption peaks, which would indicate the formation of C-O bonds. However, minor changes in the proportions of peaks intensities refer to the degradation of the polymers.

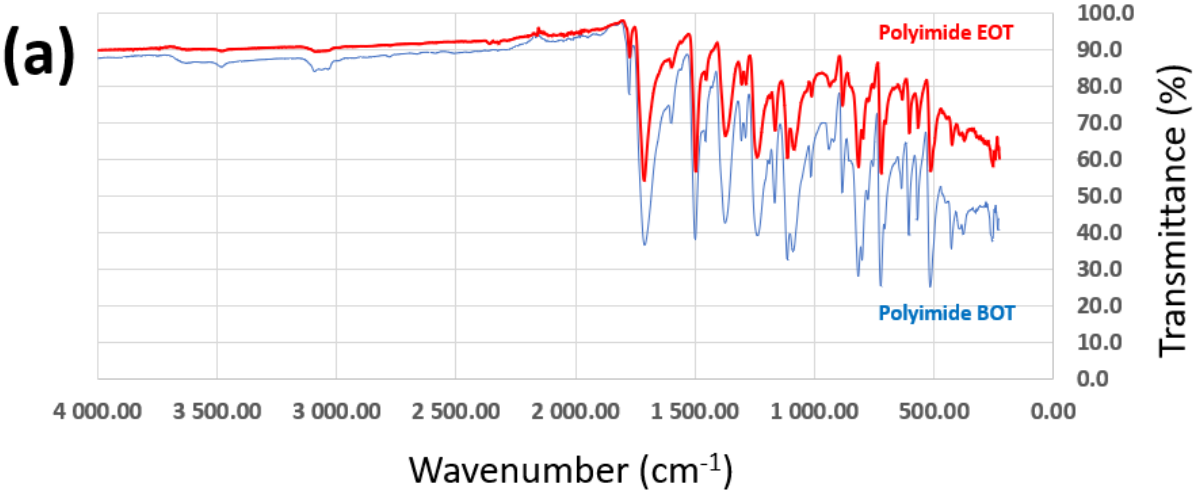

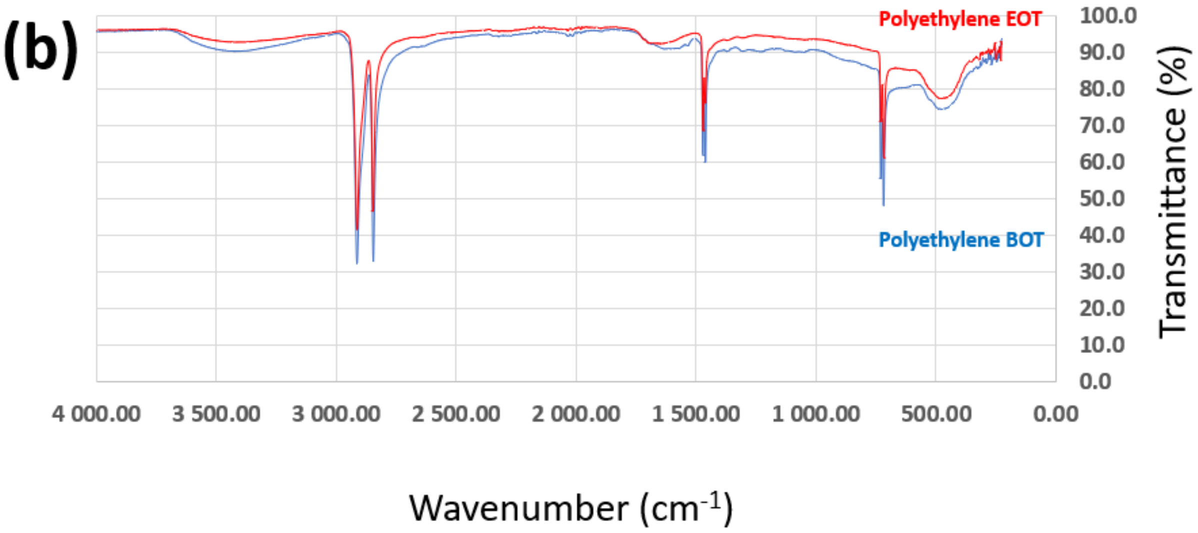

Figure. 2. Infrared spectroscopy studies of polyimide (a) and polyethylene (b) before (BOT) and after (EOT) exposure to ATOX.

The effect of energetic atomic oxygen on the elemental composition of uncoated substrates was investigated by WD-XRF and SEM-EDX, having the results summarized in Table 3. The analysis of polyimide shows that the overall elemental composition remains the same after the exposure which suggests that a layer of corrosion products does not form on the surface. This finding is in good agreement with IR spectroscopy studies (Fig. 2a). In the case of CFRP, the content of oxygen decreased, which is likely caused by the erosion of the adhesive and increased exposure of the carbon fibers. The exposure of the IR window to atomic oxygen increased the content of oxygen and zinc in its top layer. In contrast, the content of carbon had decreased.

Table 3. The elemental analysis of substrates before (BOT) and after (EOT) exposure to atomic oxygen. Less significant low content elements are not shown in the table.

Samples	Elements					
	C	O	N	Zn	Cu	Ag
Polyimide BOT	62.9	26.6	10.5			
polyimide EOT	63.0	28.7	8.3			
CFRP BOT	81.4	10.2	8.4			
CFRP EOT	86.9	5.61	7.5			
PCB BOT[a]	7.5	3.2			69.1	20.2
PCB EOT[a]	5.3	1.2			81.7	11.9
IRW BOT	96.8	2.7		0.5		
IRW EOT	82.6	16.7		0.8		

[a] The elemental composition of the metal part of the PCB was measured by SEM-EDX may be inaccurate due to the inhomogeneous nature of the alloy surface. Other substrates were studied by WD-XRF.

In order to gain a deeper insight into the corrosion effects on the IR window, additional SEM-EDX studies were done at the edge of the region exposed to ATOX (Fig. 3). The secondary electron image depicted in Fig. 3a clearly shows which region had been exposed and which part had been masked during the ATOX test. In the border region, EDX was used to map the distribution of C, O and Zn (Fig. 3b–d). These maps show that exposure to atomic oxygen had increased the content of O (Fig. 3c) and Zn (Fig. 3d), which is in good agreement with WD-XRF studies (Table 3).

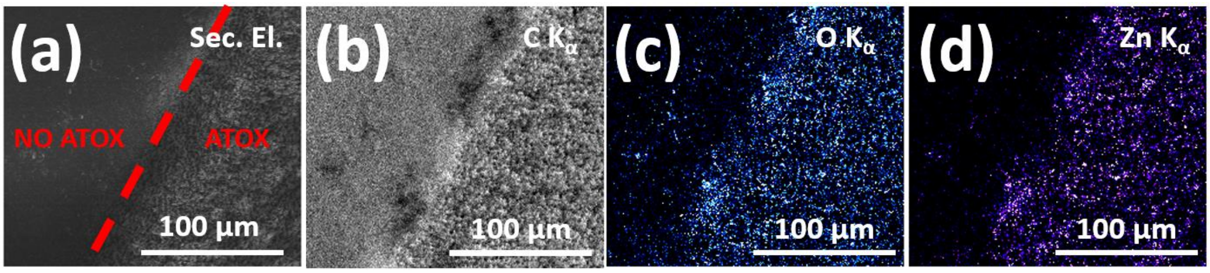

Figure 3. SEM-EDX studies of IR window at the edge of the region that was tested with atomic oxygen depicting the secondary electron image (a) and the distribution of C (b), O (c) and Zn (d).

SEM-EDX was also used to study the complex corrosion behavior of the PCB by mapping the distribution of Cu, Ag, O, C, Al, Si and Mg at the edge of the region that was tested with atomic oxygen (Fig. 4). The damage to the metal part seemed to be negligible (Fig. 1g, k) and the measurements were likely inaccurate due to the inhomogeneous nature of the surface (Table 3). However, a minor change was observed in the maps of Cu (Fig. 4b) and Ag (Fig. 4c). After the ATOX exposure the content of Cu had decreased and the content of Ag increased. A more distinct change was observed in the supporting polymer, where the exposure to atomic oxygen reduced the content of C (Fig. 4e) and increased the content of O (Fig. 4d), Si (Fig. 4g) and Mg (Fig. 4h).

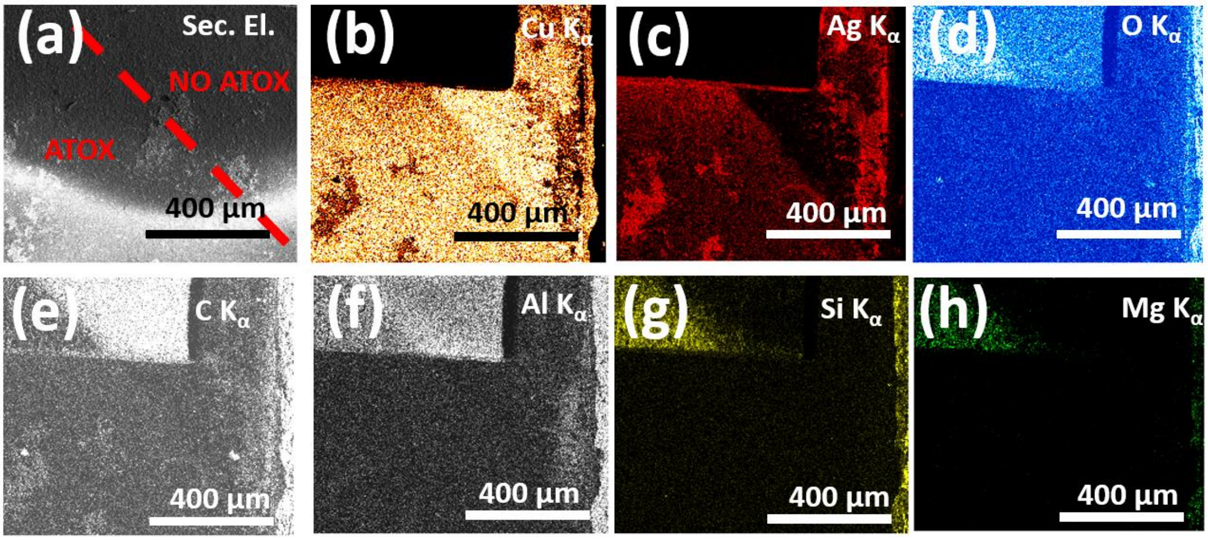

Figure 4. SEM-EDX studies of PCB at the edge of the region that was tested with atomic oxygen depicting the secondary electron image (a) and distribution of Cu (b), Ag (c), O (d), C (e), Al (f), Si (g) and Mg (h).

A more detailed study was performed to investigate the effect of atomic oxygen on the ceramic coatings grown by ALD on Si substrates as no change in visual appearance was observed. For that purpose, HR-SEM was used first, which revealed that exposure to atomic oxygen had slightly modified the top layer of the coating by introducing small ~10 nm in diameter cavities (Fig. 5). Overall, the coating appeared to be intact. Ellipsometry studies showed that the thicknesses of the ALD coatings of 22 nm did not change within measurable tolerances of +/- 1 nm. (The original coating run consisted of 5 samples, which of 2 were ATOX treated and 3 were kept as refences, all showing thickness of 22 ±2 nm). Exact measurement error from ellipsometer is hard to define, analytical error in ellipsometer model was <0.1nm. This suggests that the coating had suffered only negligible damage, similarly to the nanolaminate in an earlier study [7]. Therefore, the only notable change was in the roughness of the surface, which was in AFM studies 0.41 nm before and 0.62 nm after exposure to atomic oxygen.

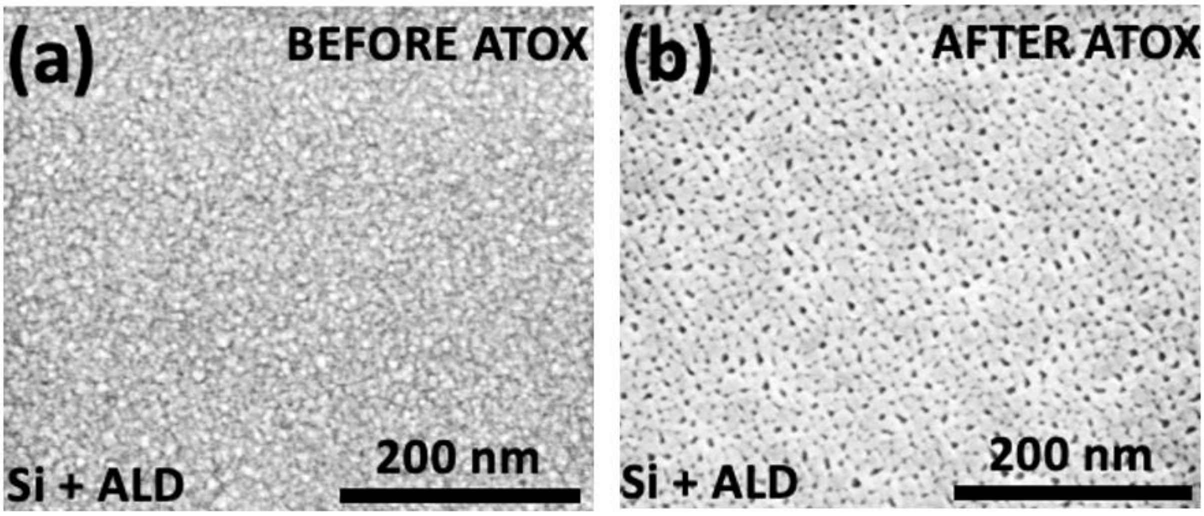

Figure 5. HR-SEM images of metal oxide coating made by ALD on Si substrate before (a) and after (b) testing with atomic oxygen.

The reflectance spectra measured for Si substrates with metal oxide coatings show that exposure to atomic oxygen slightly reduced the reflectance (Fig. 6). At shorter wavelengths, this effect could be attributed to the increase of surface roughness, which was confirmed by the AFM and HR-SEM studies (Fig. 5). However, the most dominant decrease in reflectance occurs at the infrared portion of the spectrum.

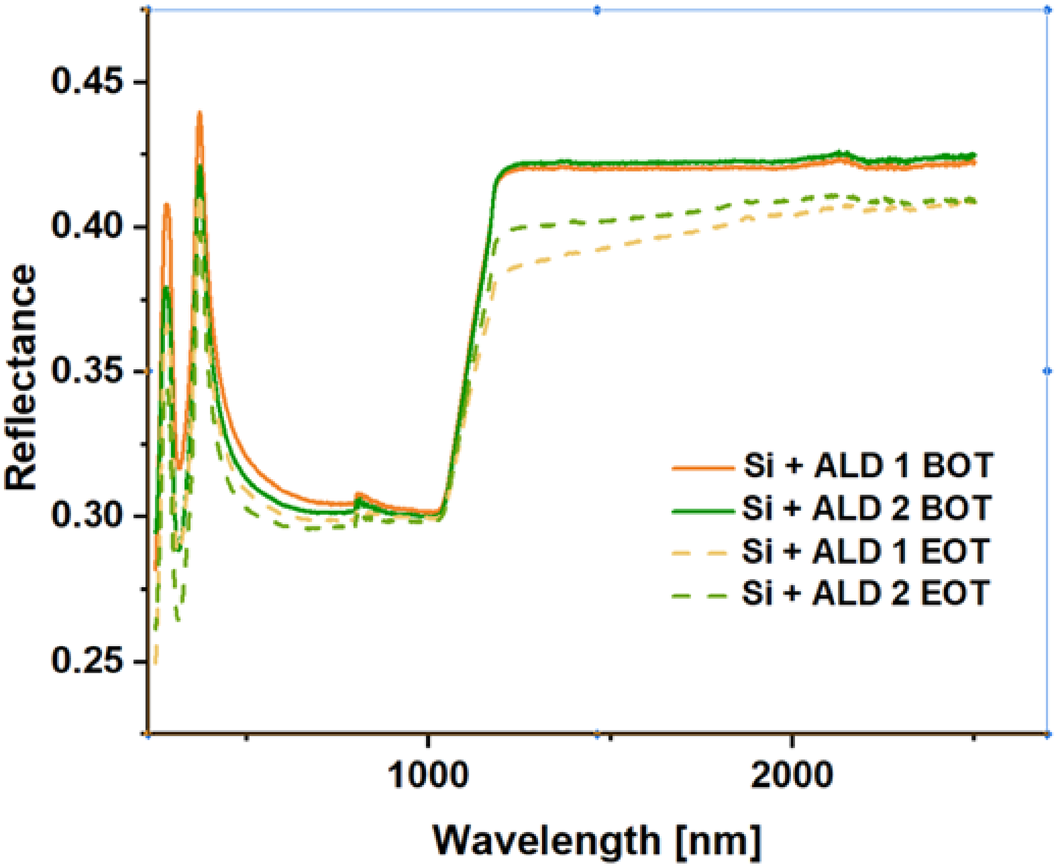

Figure 6. Reflectance spectrum of Si substrates with identical metal oxide coating grown by ALD before and after exposure to atomic oxygen. The atomic oxygen fluence for the samples is given in Table 1.

3.2. *Protection of materials with ceramic coatings grown by ALD*

The photos of substrates with ceramic coatings after exposure to atomic oxygen are depicted in Fig. 7. As can be seen from these photos, the ceramic coating successfully protected polyimide (Fig. 7a), CFRP (Fig. 7b), PCB (Fig. 7c) and the IR window (Fig. 7d) against energetic atomic oxygen, which can be regarded as significant improvement in comparison with the uncoated substrates (Fig. 1). This result is also in agreement with the HR-SEM (Fig. 5), ellipsometry and AFM studies, which showed that the ~20 nm coating protection is highly effective against ATOX erosion effects

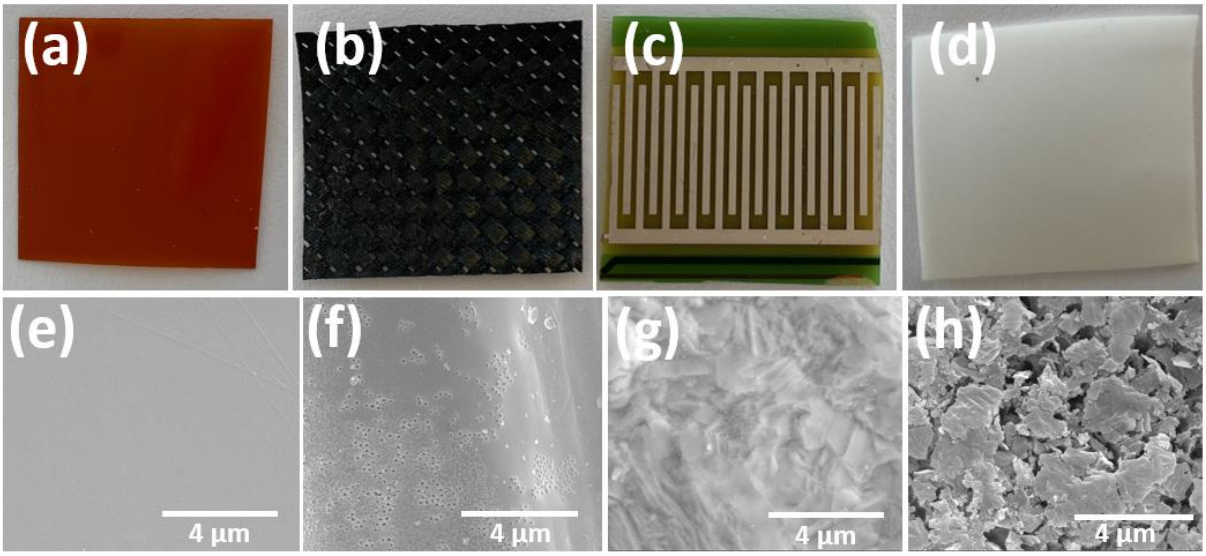

Figure 7. Photos (a-d) and SEM images (e-h) of substrates with ALD-based metal oxide coating after exposure to atomic oxygen depicting polyimide (a,e), CFRP (b,f), PCB (c,g) and IR window (d,h).

The mass measurements of coated substrates show that the use of ceramic coatings grown by ALD can significantly reduce the erosion caused by atomic oxygen (Table 4). For instance, the mass erosion of polyimide with ceramic coating was only 0.137 mg, which is over two orders of magnitude lower than the mass erosion measured for the uncoated polyimide substrate (Table 2). The lowest change was observed with the PCB, where the mass erosion value of the coated sample is reduced by a third compared to the one of the uncoated samples (Table 2,4), which is still a significant improvement of performance.

Table 4. Mass measurements of coated substrates before and after exposure to atomic oxygen.

Measured parameters	**Materials**				
	Polyimide+ALD	**CFRP+ALD**	**PCB+ALD**	**IRW+ALD**	**Si+ALD**
Mass before test (mg)	82.662	59.705	1032.951	141.478	440.147
Mass after test (mg)	82.525	58.711	1031.818	140.870	440.144
Erosion (mg; %)	0.137 (0.2%)[b]	0.994 (1.6%)	1.133 (0.1%)	0.608 (0.4%)	0.003 (0.0%)
Fluence (Atoms/cm^2, %)	2.35E+21 (266%)	2.52E+21 (286%)	1.20E+21 (136%)	1.04E+21 (118%)[a]	2.23E+21 (253%)

[a] Normalization of the fluence level, see Table 1.
[b] Normalized erosion, see Table 1.

The reflectance spectra of bare and coated substrates before and after exposure to atomic oxygen are depicted in Fig. 8. These measurements show that the reflectance of unprotected polyimide (Fig. 8a), CFRP (Fig. 8b) and PCB (Fig. 8c) drops after exposure to atomic oxygen, which is likely caused by corrosion induced surface roughness (Fig. 1i–l). In contrast, the same substrates with ceramic coating showed no significant change in reflectance after the atomic oxygen test (Fig. 8a–c). Despite the visible

corrosion effects observed in Fig. 1d,l, the reflectance of the uncoated IR window did not change much after exposure to atomic oxygen. Similarly, the use of ceramic coating on the IR window only had a negligible effect on its reflectance spectrum (Fig. 8d).
Overall, the reflectance measurements were in a good agreement with the visual inspection (Fig. 7) as well as with the mass measurements, showing that the ceramic coatings can assist in retaining the original condition of functional materials.

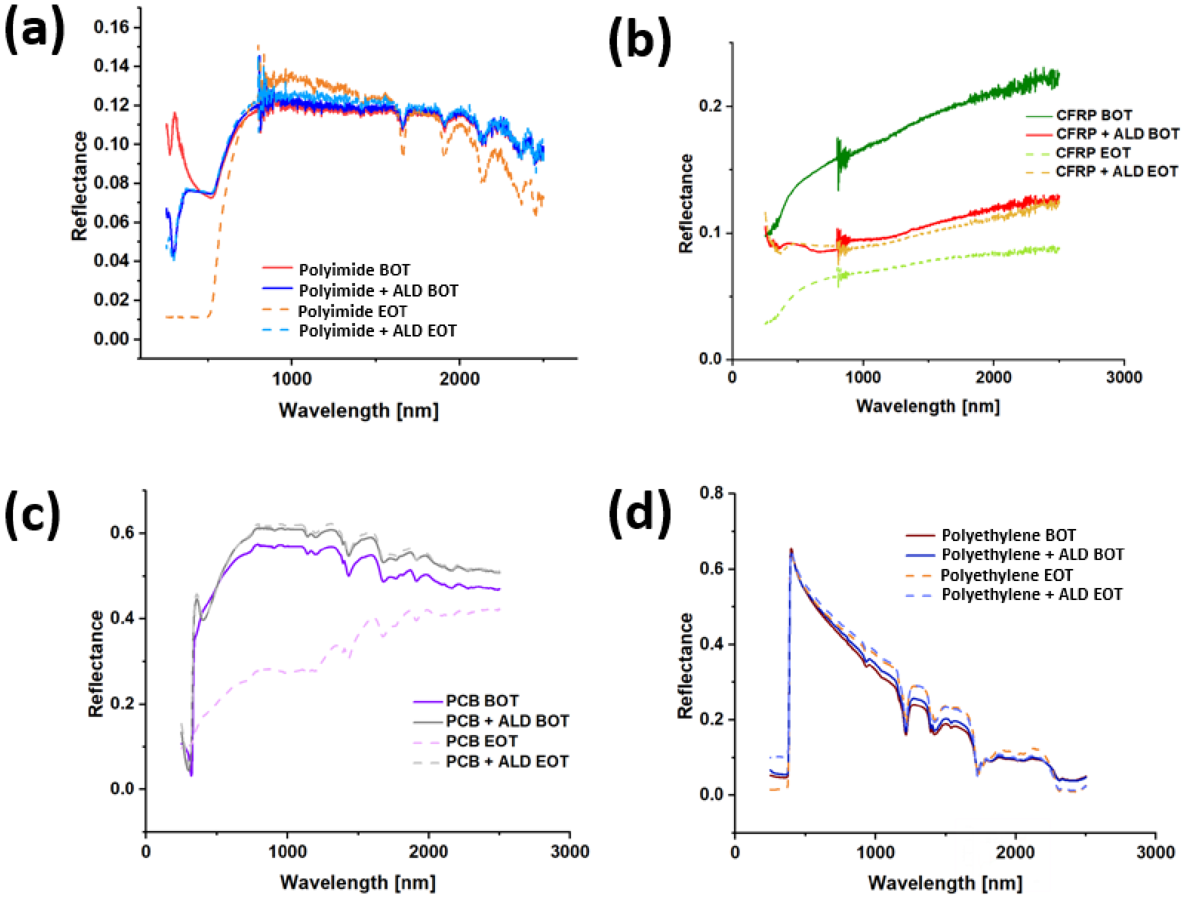

Figure 8. Reflectance spectra of bare and ALD coated polyimide (a), CFRP (b), PCB (c) and IR window (d) before (BOT) and after (EOT) exposure to atomic oxygen.

HR-SEM studies of ALD coated polyimide and IR window materials after testing with atomic oxygen revealed spatially separated sites, where the coating coverage was discontinued (Fig. 9a–d). The shape of these areas (Fig. 9a,c marked with arrows) suggested that the ALD coating cover was mechanically damaged during sample handling prior to testing with atomic oxygen. Images taken at greater magnification (Fig. 9b,d) allowed one to conclude that these coating discontinuities do not grow much when exposed to atomic oxygen. The likely explanation could be that the polymers would be damaged only after exposure to a direct flux of atomic oxygen. Undercutting likely happens but its scale is negligible, so the tests suggest that it does not have an impact in practical applications when dealing with larger parts.

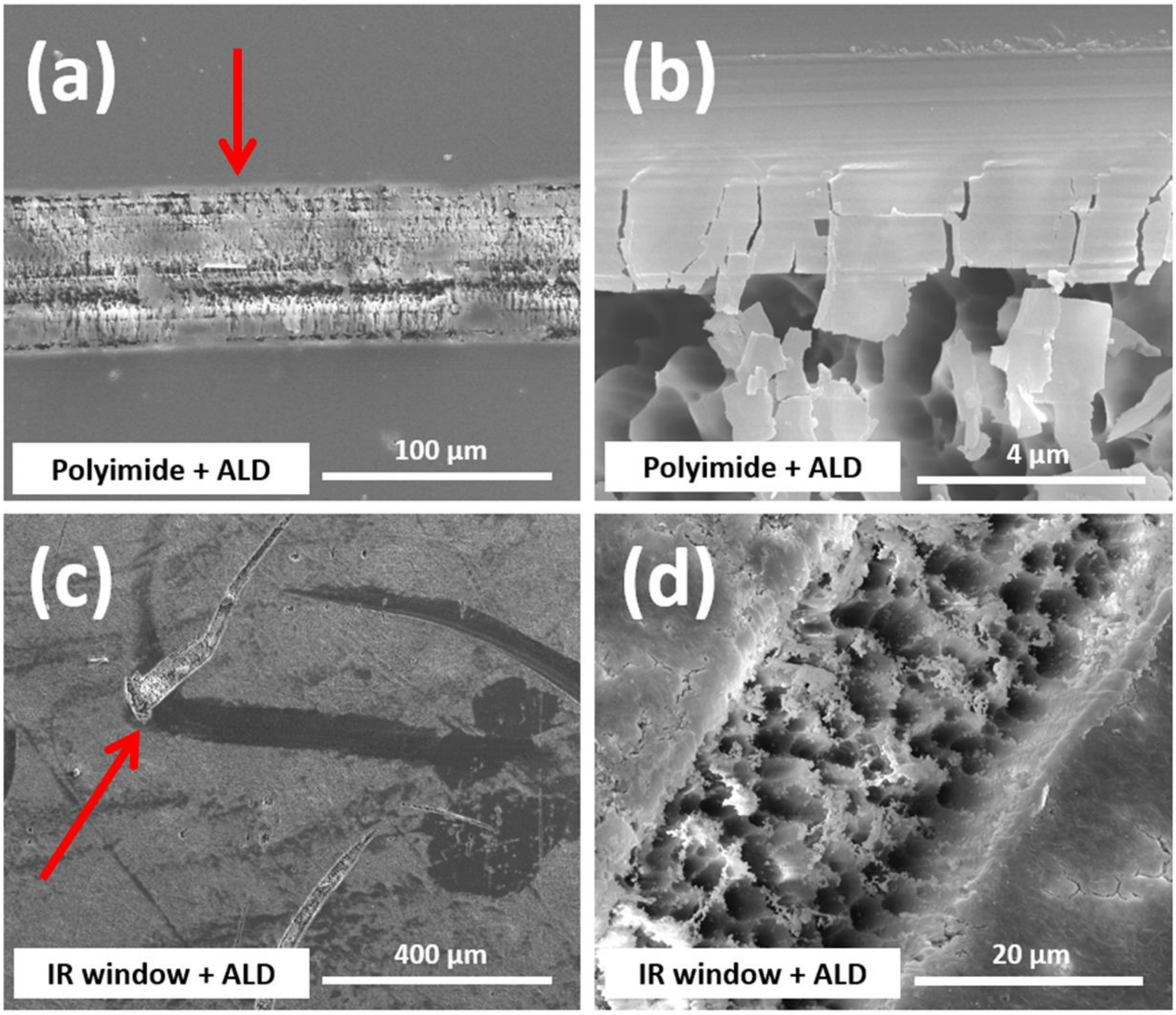

Figure 9. HR-SEM studies of corrosion on polyimide (a,b) and IR window (c,d) caused by atomic oxygen in sites where the coating had been locally damaged.

4. Discussion

4.1. Corrosion mechanism

The characterization of samples before and after exposure to atomic oxygen in this study showed that the corrosion mechanism is uniquely characteristic for each material. Generally, corrosion involves the oxidation of materials, the formation of corrosion products and typical carpet-like surface structure.

4.1.1. The effect of atomic oxygen on polyimide. In the case of polyimide, the exposure to energetic atomic oxygen causes a rather uniform erosion of the material, which results in a rough pattern with cavities on its surface also observed in an earlier study [11]. The pattern exhibits a carpet-like structure typical for ATOX erosion and is likely caused by the internal structure of polyimide, making some regions more prone to erode than others. As no increase of oxygen was observed in the composition of polyimide during the test (Table 3), it is clear that the main corrosion product was gas phase CO, which immediately leaves the surface upon formation. Therefore, the gradual oxidation results in the erosion of the material. However, the exact erosion process could not be observed with infrared spectroscopy as the method collects average data from a depth of several microns of the surface while the depolymerization process likely takes place in a nanometric depth.

4.1.2. The effect of atomic oxygen on CFRP. Similarly to polyimide, the exposure of CFRP to energetic atomic oxygen caused a rather uniform erosion of the material, where the main corrosion product is likely gas phase CO which leaves the surface upon formation. However, in the case of CFRP, the material consists of two components which are apparent to corrode at a slightly different rate. According to HR-SEM studies, the fibers (Fig. 10a) are less vulnerable to atomic oxygen than the binding material (Fig. 10b).

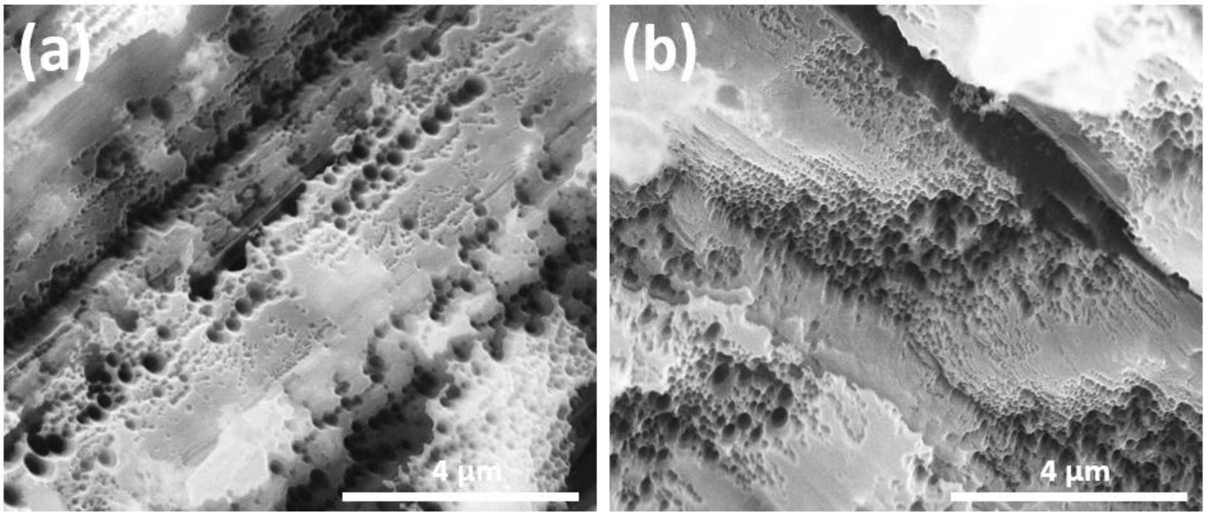

Figure 10. HR-SEM studies of CFRP after exposure to atomic oxygen depicting the fibers (a) and the binding material (b).

4.1.3. The effect of atomic oxygen on PCB. The green solder mask, as well as the metal part of the PCB both suffered damage from atomic oxygen (Fig. 1k, Fig. 4). Generally, for PCBs, the metal part is most critical for the operation of an electronic system and according to EDX studies it consists mainly of copper and silver (Table 3). SEM-EDX studies (Fig. 4) demonstrated that the metal part is less vulnerable to atomic oxygen than the support material, which also explains why the overall erosion of PCB was lower than the erosion of polyimide or CFRP (Table 2). Due to the deterioration of both the metal as well as the green solder mask, a protective coating may still be needed on a PCB when used in LEO. That's because in this study the atomic oxygen test simulated only 1 year of exposure to space in LEO, which already introduced damage to the surface of the PCB. However, in practical applications the duration of a mission can be several years and during that time the damage would accumulate.

4.1.4. The effect of atomic oxygen on IR window. The corrosion of the IR window is somewhat similar to that of polyimide and CFRP, where the dominant corrosion product seems to be gaseous CO. However, the increase in the oxygen content in the elemental composition of the IR window after testing suggested that some amount of the oxygen has either constituted solid corrosion products or was physically trapped on the surface region. Such trapping may happen if the atomic oxygen particles interact with each other inside the polymer and form O_2 and/or H_2O which are less likely to escape the material. The IR window contains a certain amount of zinc, which may easily oxidize (to a solid corrosion product) and contribute to the overall increase in the oxygen content. However, the amount of zinc was relatively low, which implied that it cannot be solely responsible for the significant/high increase of the oxygen content. Furthermore, the spectra in the IR range are nearly identical before and after testing, which suggests that oxygen has not been chemically bound to carbon in the polyethylene chains. However, X-ray photoelectron spectroscopy studies carried out and reported in an earlier paper [12] allowed one to conclude that some oxygen may become chemically bound to polyethylene, which can partly explain the increase of oxygen content seen also in the present WD-XRF studies (Table 3).

Finally, the relevant bonds would only form in the very top layer of the IR window, making it too small to be observable in infrared spectroscopy studies.

4.1.5. The effect of atomic oxygen on the ceramic coating made by ALD. The ceramic coating investigated in this study is a metal oxide by nature. Therefore, theoretically, it would be impossible for the coating material to chemically bind additional oxygen in conditions used in this work, effectively making it corrosion resistant in an oxidizing environment. However, it should be mentioned here that oxygen vacancies in the ceramic coating could still be filled with oxygen. This could have an effect on the conductivity of the coating but not the overall corrosion resistance. The effect of atomic oxygen on the conductivity of ceramic coatings may be relevant for mitigating surface charging related issues. Another component of the corrosion process would likely be the physical erosion during the interaction of the material with atomic oxygen but the kinetic energy of atomic oxygen cannot possibly be very high. This might explain why in the HR-SEM studies of the present work (Fig. 5) as well as in a paper published earlier [7], the damage caused to the ceramic coating by atomic oxygen remained negligible and affected only the top layer. This damage may have been caused by physical sputtering, where some of the coating material may also be redeposited on the surface. This would also explain why the thickness of the ultra-thin ceramic materials does not change when exposed to atomic oxygen. However, the exposure to atomic oxygen did lower the reflectance of the coating, which can possibly be explained by the changes in surface roughness, refractive index and optical absorption, somewhat speculatively also the electrical properties. In particular, the reduction of reflectance at lower wavelengths can quite likely to be attributed to the increase in surface roughness and the decrease in average refractive index. At higher wavelengths, the reduction of reflectance may be caused by the increase of electrical resistance according to Drude model [13] and/or due to higher absorption in the infrared region due to vibrational excitations.

4.2. The protection efficiency of ceramic coatings grown by ALD

The good protection efficiency of ceramic coatings on different substrates investigated in this study can be explained by the chemical inertness of the coatings towards atomic oxygen, the ability to coat uniformly the whole surface by ALD, and a good adhesion of the coating to the underlying substrate. Even so, some erosion was observed in the mass measurements (Table 4), which could be attributed to localized sites where the coating coverage was disrupted or damaged during the sample handling (Fig. 9). One can, possibly, overcome this in practical applications, where the coating preparation methodology has to be optimized for specific materials, using appropriate pre-treatments and coating synthesis parameters for the chosen ALD process. Furthermore, the handling procedures of substrates in practical applications can be developed, which should improve the overall quality of the coating. Additionally, even if the coatings were damaged, it is unlikely that delamination due to the corrosion of underlying atomic oxygen would take place and, therefore, the majority of the materials surface would still be sufficiently protected. Nonetheless, what has not been covered in this study are the effects of cyclical of temperature fluctuations and exposure to ionizing radiation in combination with energetic atomic oxygen. These synergistic effects may lead to an enhanced delamination of the ceramic coatings on polymers but this needs to be studied further.

5. Conclusions

In this study we demonstrated that ultra-thin ceramic coatings grown by ALD can enhance the corrosion resistance of polyimide, CFRP, PCB and the IR window substrates against energetic atomic oxygen.

Our studies with the bare substrates not covered by ALD coatings, at first, provided deeper insight into the corrosion mechanism of different materials when exposed to atomic oxygen. The studies indicate that in the case of polyimide, CFRP and IR window, the dominant corrosion product is most likely volatile CO in gaseous form. As a result, polymer materials gradually eroded under the flux of atomic oxygen and passivating films on such materials were not formed. However, on the microscopic scale, such erosion occurred unevenly, which resulted in a carpet-like, rough surface structure and, consequently in a decreased of the reflectivity. The uneven erosion was most notable in the case of CFRP, PCB and IR window which consisted of two different (raw) materials. In the case of CFRP, the binding material eroded faster than the carbon fibers. With regards to the PCB, the metal parts suffered little damage while the green support material was depleted of carbon and exhibited an increase of oxygen. In the case of the IR window, the erosion of carbon-based polyethylene exposed Zn particles which were originally in the composite material.

The use of ceramic coatings on polyimide, CFRP, PCB and the IR window reduced the rate of erosion by a factor of over 100, which means a significant improvement in the respective material's corrosion resistance. Furthermore, the coating's corrosion prevented the material's degradation with regards to the reflectance spectra over a broad spectral range.

The useful performance of the ceramic coating mainly lies in its chemical inertness against atomic oxygen, assisted by a good adhesion to the substrates and the natural advantage of ALD to uniformly coat the whole substrate surface compared to other coating techniques. As a result, the ceramic coating has, in the present study, hindered the oxidation of carbon by energetic atomic oxygen on the surface of the studied materials and therefore effectively prevents corrosion. HR-SEM studies showed that the very surface of the coating was slightly damaged after the atomic oxygen exposure, however the overall thickness of the coating remained unchanged as confirmed by the ellipsometry measurements. Furthermore, ceramic coatings did not delaminate even in areas with defects when exposed to atomic oxygen flux. This means that the majority of the substrate surface remained protected even if the coating suffered some mechanical damage during handling.

The findings of this study suggest that the use of ceramic coatings made by ALD may become highly useful and suitable for enhancing the performance of various materials in low Earth orbit applications. In addition, the results may lead to broadening of the list of materials that can be used in space.

6. References

[1] de Rooij A 2010 Corrosion in space *Encyclopedia of Aerospace Engineerings* ed Blockley R and Shyy (Wiley) W
https://onlinelibrary.wiley.com/
https://onlinelibrary.wiley.com/doi/abs/10.1002/9780470686652.eae242
http://esmat.esa.int/publications/published_papers/corrosion_in_space.pdf;
Last visited in August 2022.

[2] de Groh K K, Banks A B, Dever J A, Jaworske D A, Miller S K, Sechkar E A and Panko S R 2008 NASA Glenn Research Center's Materials International Space Station Experiments (MISSE 1-7). *NASA/TM-2008-215482*
https://ntrs.nasa.gov/api/citations/20090005995/downloads/20090005995.pdf

[3] de Groh K K and Banks B A 2019 Atomic oxygen erosion data from the MISSE 2-8 missions. *NASA/TM-2019-219982*
https://ntrs.nasa.gov/api/citations/20190025445/downloads/20190025445.pdf

[4] ESA-ESTEC LEOX Facility
https://esamultimedia.esa.int/multimedia/industry/ESA_TECQE_AO_013375.pdf

[5] Matero R, Ritala M, Leskelä M, Salo T, Aromaa J and Forsen O 1999 Atomic layer deposited thin films for corrosion protection. J. Phys. IV France 9 pp 493–499. https://doi.org/10.1051/jp4:1999862

[6] Ritala M and Leskelä M 2002 Atomic layer deposition. *Handbook of Thin Films* **1** pp 103–159. https://pubs.acs.org/doi/10.1016/B978-012512908-4/50005-9

[7] Merisalu M, Aarik L, Piirsoo H M, Kozlova J, Tarre A, Zabels R, Wessing J, Brieva A and Sammelselg V 2022 Nanostructured coating for aluminum alloys used in aerospace applications.

Journal of the Electrochemical Society **169** https://iopscience.iop.org/article/10.1149/1945-7111/ac7bb2

[8] Smith C T G, Delkowki M, Anguita J V, Cox D C, Haas C and S Ravi P Silva 2021 Complete atomic oxygen and UV protection for polymer and composite materials in a low Earth orbit ACS *Applied Materials and Interfaces* **13** pp 6670-6677 https://pubs.acs.org/doi/10.1021/acsami.0c21552

[9] Kestilä A, Nordling K, Miikkulainen V, Kaipio M, Tikka T, Salmi M, Auer A, Leskelä M and Ritala M 2018 Towards space-grade 3D printed, ALD-coated small satellite propulsion components for fluidics *Additive Manufacturing* **22** pp 31-37 https://doi.org/10.1016/j.addma.2018.04.023

[10] Jen S H, Bertrand J A and George S M 2011 Critical tensile and compressive strains for cracking Al_2O_3 films grown by atomic layer deposition *AIP Journal of Applied Physics* **109** 084305 http://dx.doi.org/10.1063/1.3567912

[11] Banks B A, Rutledge S K, Hunt J D, Drobotij E, Cales M R and Cantrell G 1995 Atomic oxygen textured polymers *NASA Technical Memorandum* **106769**

[12] Zafar R, Park S Y and Kim C G 2021 Surface modification of polyethylene microplastic particles during the aqueous-phase ozonation process *Environmental Engineering Research* **26(5)** 200412 https://doi.org/10.4491/eer.2020.412

[13] Drude model: https://en.wikipedia.org/wiki/Drude_model

Acknowledgments

The authors thank dr. Aarne Kasikov for fruitful consultations in the interpretation of optical measurements and Peeter Ritslaid for the assistance in X-ray fluorescence spectroscopy studies. The studies were partly funded by the EU through the European Regional Development Fund under project TK141 (2014-2020.4.01.15-00). The atomic oxygen testing was performed in the framework of the "Announcement of opportunity for atomic oxygen in the ESTEC Materials and Electrical Components Laboratory/ESA-TECQE-AO-013375)," through a collaboration with Picosun Oy.